ELSEVIER

Journal of Power Sources 74 (1998) 234–239

JOURNAL OF POWER SOURCES

Short communication

A method to monitor valve-regulated lead acid cells

A.K. Shukla [a,*], V. Ganesh Kumar [a], N. Munichandraiah [b], T.S. Srinath [c]

[a] *Solid State and Structural Chemistry Unit, Indian Institute of Science, Bangalore-560 012, India*
[b] *Department of Inorganic and Physical Chemistry, Indian Institute of Science, Bangalore-560 012, India*
[c] *Amara Raja Batteries, Karakambadi, Tirupati-517 520, India*

Received 1 December 1997; accepted 16 January 1998

Abstract

The individual electrode impedance parameters and internal resistance of industrial type 120-Ah valve-regulated lead acid (VRLA) cells are obtained from a galvanostatic nondestructive technique. The resistive components of the cells are found to be minimum at a state-of-charge (SOC) value of 0.5. The study reflects that the optimum performance of the VRLA cells is achieved at SOC values between 0.2 and 0.8.

Keywords: Valve-regulated lead acid cells; Impedance; State-of-charge

1. Introduction

In recent years, conventional flooded-type lead acid batteries are replaced by maintenance-free VRLA systems, particularly in telecommunications, automotive and standby applications [1–5]. This is because the VRLA batteries offer the freedom of cell placement, cycleability without the need for the addition of water or checking the specific gravity, increased safety, and superior performance in some instances [6]. The sealed configuration of VRLA batteries makes it mandatory to find surveillance techniques for power-system reliability in these applications [7]. As part of our ongoing research in this area [8,9], this communication reports a galvanostatic technique for monitoring electrode impedance and internal resistance of 120-Ah VRLA cells that are central to their performance. The steep rise in the positive electrode impedance as the state-of-charge (SOC) of the VRLA cells approaches unity is attributed to: (a) the positive-limited operation of the cells; (b) the charge-transfer resistance of the sluggish oxygen evolution reaction on PbO_2 electrode.

2. Experimental

VRLA cells with 120-Ah rated capacity (C) and a nominal voltage of 2 V, obtained from Amara Raja Batteries (India), were conditioned by conducting five charge–discharge cycles at the $C/10$ rate. The fully conditioned batteries were found to yield a faradaic efficiency of about 80%. The cells were charged to 120% of their rated capacity, and then discharged to a cut-off voltage of 1.7 V. The electrical circuit employed during the present studies is shown in Fig. 1. It consists of the test cell, a decade resistance box, a regulated dc power supply and a microswitch. The technique involves discharge of the test cell at a substantially low rate ($C/700$) and necessitates precise measurement of concomitant changes in voltage. The voltage of the test cell was therefore required to be compensated by another cell of the same type. The measurement of compensated voltage (V) of the test cell at any instance with respect to its rest value (V_r), i.e., $V - V_r$, is achieved through a high input impedance Solartron-7150 digital multimeter interfaced to an IBM-PC through an IEEE-488 BUS. The data acquisition was carried out through a program written in GW-BASIC. The data were collected at intervals of 0.5 s over a duration of 450 s. All the experiments were performed at 24($\pm$1)°C. The noise level in the collected data was within ± 2 μV. The data were further smoothened with the aid of the Microcal

* Corresponding author. Tel.: +91-80-3311310; fax: +91-80-3311310; e-mail: shukla@sscu.iisc.ernet.in.

0378-7753/98/$19.00

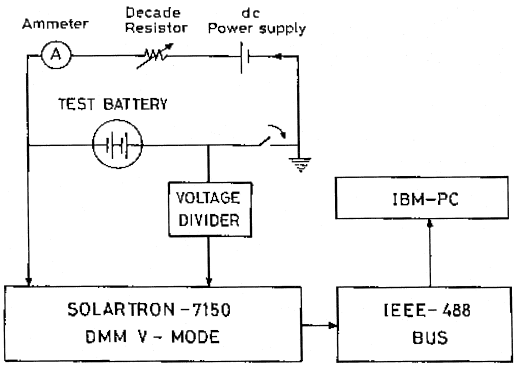

Fig. 1. Schematic diagram of setup for digital recording of $V-t$ transients.

Origin software. The data collection and analysis were carried out repeatedly at several SOC values of the test cells in order to ensure the reproducibility.

3. Results and discussion

The charge–discharge data of a test cell at the $C/10$ rate are shown in Fig. 2. The equivalent circuit of the test cell under the conditions described in Section 2 is shown in Fig. 3, where T_1 and T_2 are the cell terminals, R_Ω is the ohmic resistance. $R_{t,1}$ and $C_{d,1}$ are charge-transfer resistance and interfacial capacitance, which includes double-layer capacitance and associated capacitive components due to adsorption, passive films, etc., for one of the electrodes, and $R_{t,2}$ and $C_{d,2}$ are charge-transfer resistance and interfacial capacitance for the other electrode. As the discharge current (170 mA) corresponding to the $C/700$ rate is restricted to a duration of a couple of minutes only, the SOC of the test cell changes only by 0.00001 and

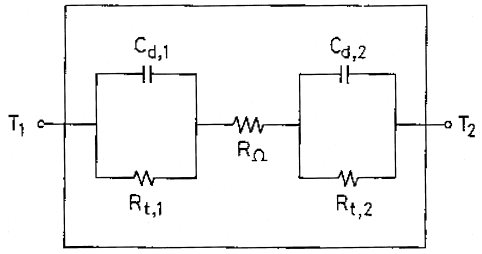

Fig. 3. Equivalent circuit for test cell.

could be taken to be nearly invariant for all practical purposes. Accordingly, it could be assumed that the electron-transfer processes are the rate-determining steps for both the electrode reactions. Since the electrode processes are not governed by mass transfer, the Warburg components are not included in the equivalent circuit [10,11].

For a small current perturbation, the voltage response of the test cell can be written with reference to the equivalent circuit shown in Fig. 3 as:

$$V_r - V = IR_\Omega + IR_{t,1}\left[1 - \exp\left(-t/\tau_1\right)\right] + IR_{t,2}\left[1 - \exp\left(-t/\tau_2\right)\right], \quad (1)$$

where I is the discharge current, $\tau_1 (= R_{t,1}\ C_{d,1})$ and $\tau_2 (= R_{t,2}\ C_{d,2})$ are the time constants of the associated electrode processes. The exponential terms in Eq. (1) are due to the charging of $C_{d,1}$ and $C_{d,2}$. At time $t > \tau_1$ and τ_2, the capacitors are completely charged and therefore the voltage drop is only due to resistive components [8–11], namely $R_{t,1}$, $R_{t,2}$ and R_Ω.

A solution of Eq. (1) provides the impedance parameters of the test cell. Since there are serious limitations in the direct algebraic procedure to solve Eq. (1), an alternative approach described below becomes imperative. This procedure employs the assumption that the time constants,

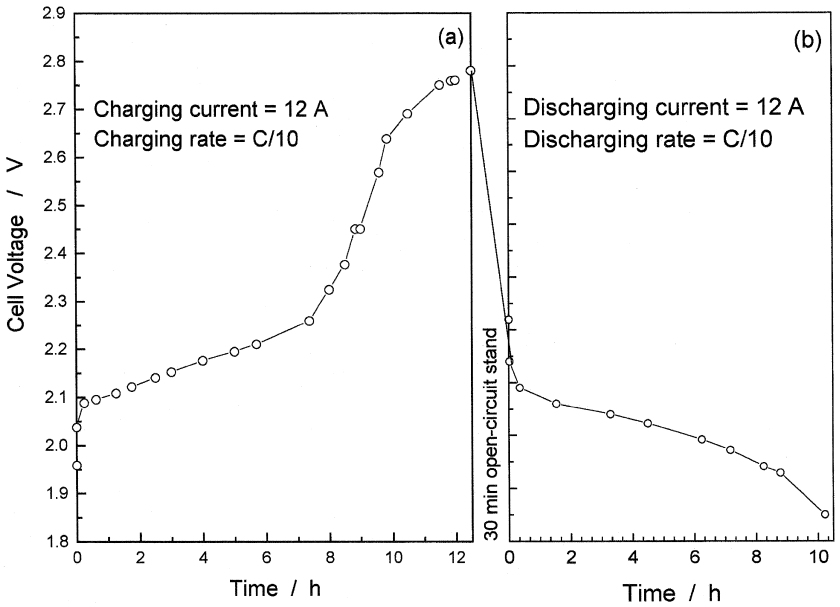

Fig. 2. Typical (a) charge (charging current = 12 A ($C/10$)) and (b) discharge (discharging current = 12 A ($C/10$)) curves for VRLA cell.

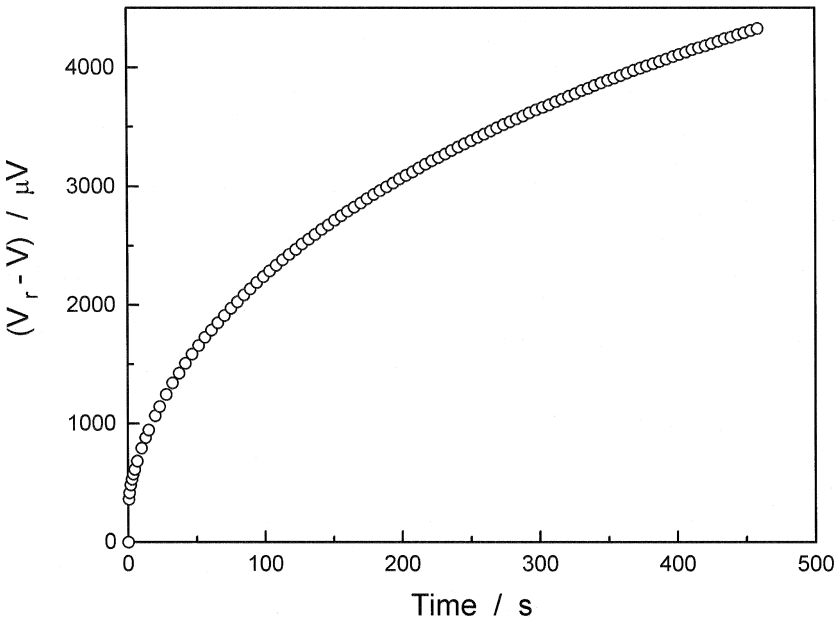

Fig. 4. Typical galvanostatic discharge transient (discharging current = 170 mA ($C/_{700}$)) of the test cell at SOC = 0.9.

τ_1 and τ_2, differ by one order of magnitude. The procedure involves the following steps.

Step 1: Eq. (1) shows that V vs. t is nonlinear. Two instances of time ($t*$ and $t**$) in the initial region of the V–t curve are chosen such that there is a measurable difference in the corresponding slopes ($m*$ and $m**$) of the curve. Although the time zone of these slopes is governed by the relaxation processes at both the electrodes, as an approximation it is assigned entirely to one of the processes, namely the τ_1-process. The approximate value of τ_1, namely τ_1', is given by:

$$\tau_1 = \frac{t** - t*}{\ln(-m*) - \ln(-m**)}, \qquad (2)$$

which is obtained by differentiating Eq. (1) with respect to time (t) and neglecting the contribution from the τ_2-process.

Step 2: Since the function $[1 - \exp(-t/\tau)]$ attains about 99% of its final value at $t = 5\tau$, it is assumed that the relaxation at $t > 5\tau_1'$ is due only to the τ_2-process.Under this condition, Eq. (1) reduces to:

$$V_r - V = I(R_\Omega + R_{t,1}) + IR_{t,1}\left[1 - \exp(-t/\tau_2)\right], \qquad (3)$$

which yields:

$$\ln(-dV/dt) = \ln(IR_{t,2}/\tau_2) - t/\tau_2. \qquad (4)$$

A linear plot of $\ln(-dV/dt)$ vs. t in the time domain $t > 5\tau_1'$ provides τ_2 and $R_{t,2}$ from its slope and intercept, and hence $C_{d,2}$. Substitution of Eq. (4) in Eq. (3) followed by a plot of $(V_r - V)$ vs. $\exp(-t/\tau_2)$ gives a straight line in the time domain $t > 5\tau_1'$. The intercept of the plot with the y-axis gives the value of the total internal resistance, $R_i(= R_\Omega + R_{t,1} + R_{t,2})$.

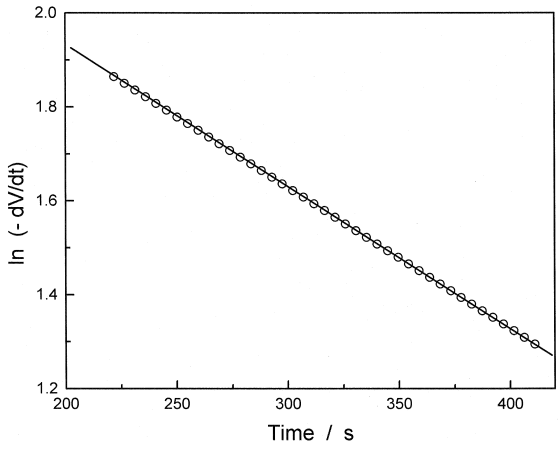

Fig. 5. Plot of $\ln(-dV/dt)$ against time at SOC = 0.9 for test cell.

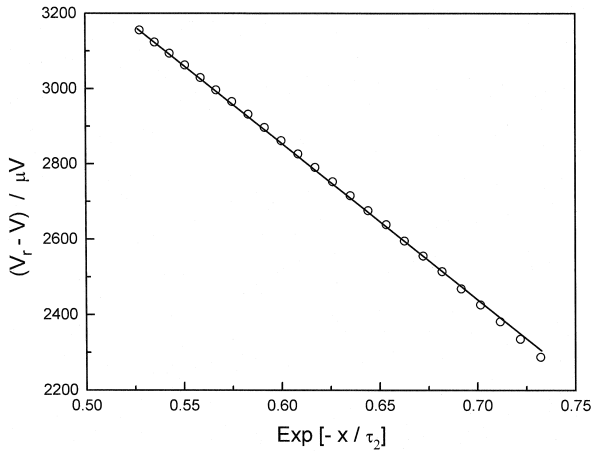

Fig. 6. Plot of $V - V_r$ against $\exp(-t/\tau_2)$ at SOC = 0.9 for test cell.

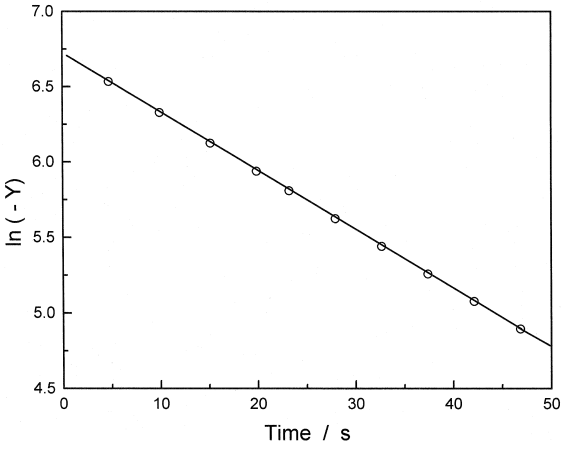

Fig. 7. Plot of $\ln(-Y)$ against time at SOC = 0.9 for test cell.

Step 3: Eq. (1) is now recast as:

$$Y = -IR_{t,1}\exp(-t/\tau_1), \quad (5)$$

where $Y = V_r - V - IR_i + IR_{t,2}\exp(-t/\tau_2)$. Therefore:

$$\ln(-Y) = \ln(IR_{t,1}) - t/\tau_1. \quad (6)$$

Since Y is now known completely at each t, a plot of $\ln(-Y)$ vs. t in the time domain $t < \tau_2/5$ gives a straight line of slope $(-1/\tau_1)$ and intercept $IR_{t,1}$. This step provides the values of τ_1 and $R_{t,1}$, and hence $C_{d,1}$. Furthermore, R_Ω can also be calculated. All the five parameters, namely R_Ω, $R_{t,1}$, $R_{t,2}$, $C_{d,1}$ and $C_{d,2}$, of the test cell are thus obtained by a low-rate galvanostatic discharge of the cell over a short duration. A typical galvanostatic discharge transient of the test cell at SOC = 0.9 for 420 s is shown in Fig. 4. The linear polarization domain in the analysis is ensured by recording transients with several discharge currents close to $C/700$ and plotting $(V_r - V)/I$ against t. All the plots lie within an error of $\pm 2\%$ in a time zone extending to 450 s and hence the data within this duration are included in the analysis.

Employing Eq. (2), τ_1' is calculated to be 30 s from the slopes of the voltage transient curve at two instants lying between 5 and 10 s. In the region $t > 5\tau_1'$ which is equal to 150 s, the plot of $\ln(-dV/dt)$ vs. t is a straight line between 200–420 s as shown in Fig. 5. From the slope and intercept of this plot, τ_2 and $R_{t,2}$ are calculated to be 332 s and 23.7 mΩ, respectively. Accordingly, $C_{d,2}$ is estimated to be 14 kF. By substituting the values of τ_2 in Eq. (3), $(V_r - V)$ is plotted against $\exp(-t/\tau_2)$ in the time domain $t > 5\tau_1'$, as shown in Fig. 6. The total resistance $R_i(= R_\Omega + R_{t,1} + R_{t,2})$ calculated from the intercept of the plot is 30.37 mΩ.

From the values of R_i, $R_{t,2}$ and τ_2, the values of Y were computed in the time domain $t < \tau_2/5$, and $\ln(-Y)$ is plotted against t, as shown in Fig. 7. From the slope and intercept, the values of τ_1 and $R_{t,1}$ are estimated to be 25.67 s and 4.69 mΩ, respectively. The capacitance $(C_{d,1})$ and internal resistance (R_Ω) thus obtained are found to be 5.47 kF as 1.94 mΩ, respectively. The resistive and reactive components of the VRLA cell have been evaluated at different SOC values and the data are presented in Figs. 8 and 9.

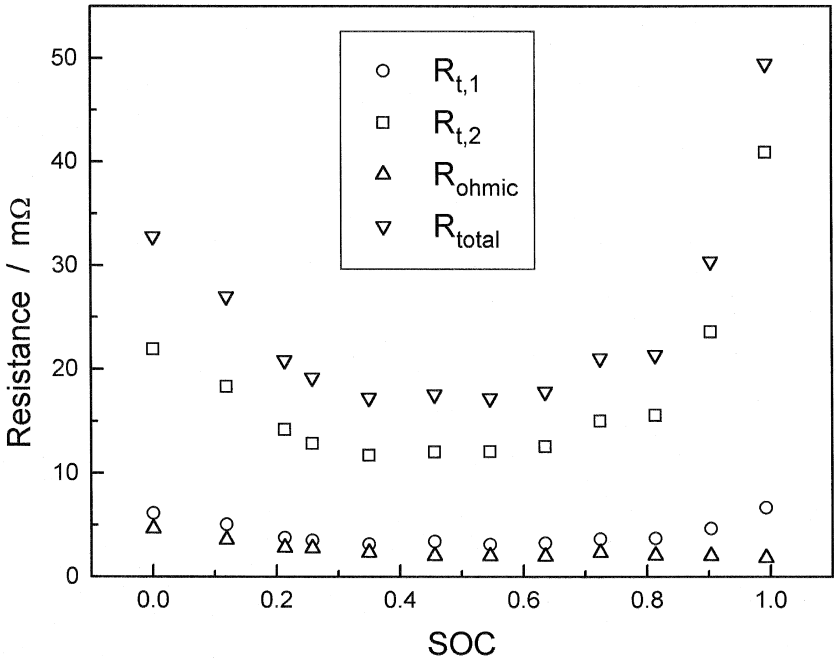

Fig. 8. Plot of resistive components of test cell as a function of SOC values.

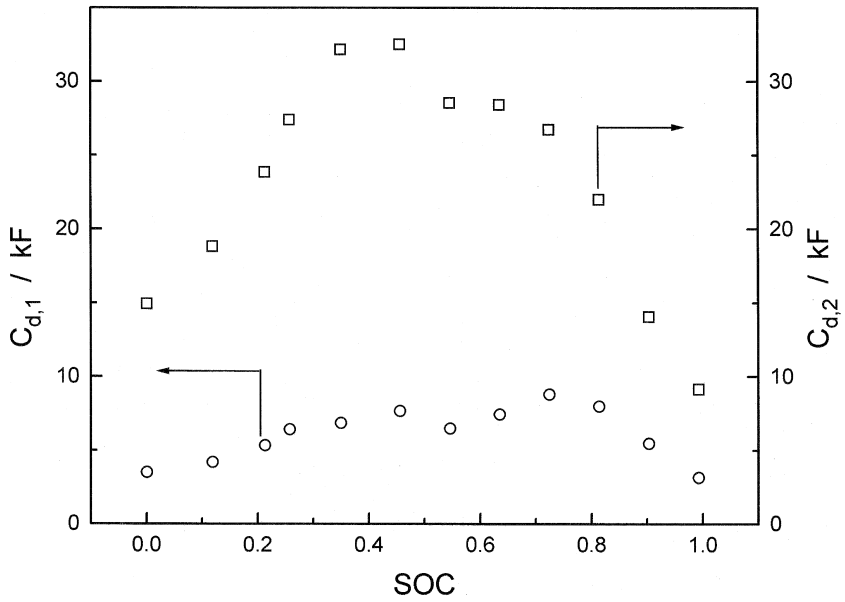

Fig. 9. Plot of capacitive components of test cell as a function of SOC values.

Electrodes 1 and 2 could be assigned as anode and/or cathode of the cell in the light of following argument. Among the two electrodes, namely, $Pb/PbSO_4$ and $PbO_2/PbSO_4$, the former has lesser charge-transfer resistance for the associated electrochemical reactions [12]. Accordingly, electrode 1 is assigned as the $Pb/PbSO_4$ electrode (anode or negative electrode) and electrode 2 as the $PbO_2/PbSO_4$ electrode (cathode or positive electrode) of the VRLA cell. It is noteworthy that the electrical conductivity of Pb is higher than PbO_2 [1].

Both the positive and negative plates of lead acid cells during the charge–discharge cycles undergo heterogeneous reactions involving two solids [13], and, therefore, their charge-transfer resistances should be invariant with change in activities of the oxidized/reduced species. Although this is reflected in the charge-transfer resistance ($R_{t,1}$) values for the negative plate over the entire range of SOC values of the VRLA cells studied here (see Fig. 8), the charge-transfer resistance ($R_{t,2}$) of the positive plate is found to increase steeply from SOC values of 0.8–1.0 (Fig. 8) Such a behaviour of the positive plate could only be attributed to the charge-transfer resistance of the sluggish oxygen evolution reaction on PbO_2 surface that leaves a layer of oxygen on the positive plate of the cell during its overcharge. This oxygen layer subsequently acts as a barrier, during the discharge of the cell, limiting its performance.

The variation in capacitance values of the anode ($C_{d,1}$) and cathode ($C_{d,2}$) with SOC values of the VRLA cells are shown in Fig. 9. Both the $C_{d,1}$ and $C_{d,2}$ values are larger than the normally reported values for electrode/electrolyte interfaces. This is quite likely due to the highly porous nature of the electrodes. In the literature [14–17], interfacial capacitance values as high as 1.5 kF have been reported for the battery electrodes. The respective relaxation times, τ_1 and τ_2, for the negative and positive

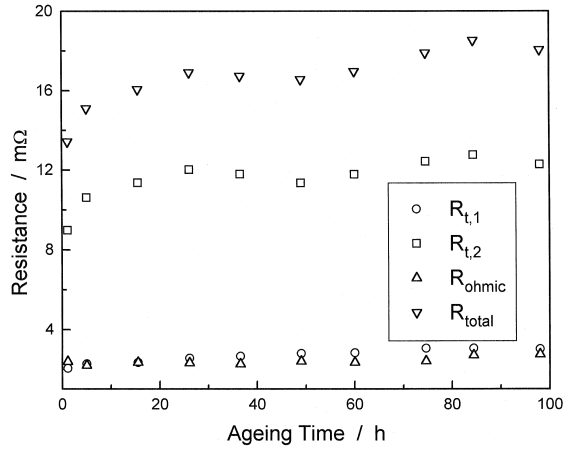

Fig. 10. Variation in resistive components of test cell with ageing time.

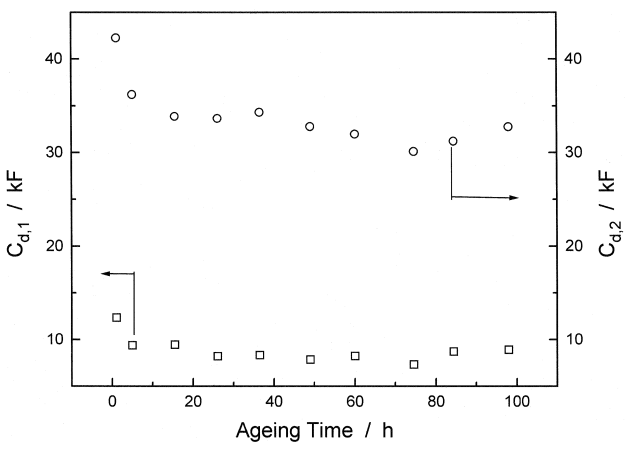

Fig. 11. Variation in capacitive components of test cell with ageing time.

electrodes are found to differ by an order of magnitude. Accordingly, the $Pb/PbSO_4$ electrode, with a smaller relaxation time value, has faster kinetics than the $PbO_2/PbSO_4$ electrode.

The evolution of the impedance parameters at a particular SOC during the open-circuit (ageing) are shown in Figs. 10 and 11. It is observed from the data that the values for the impedance parameters are stabilized only after ≈ 20 h. The charge-transfer resistances and ohmic resistances increase with the ageing time and attain a maximum after about 20 h; the interfacial capacitive components are found to be minimum over the same duration. These observations indicate that the determination of SOC values for the VRLA cells by this method would require a minimum of open-circuit stand of 20 h [18].

4. Conclusions

The data from the present study indicate that a marked variation in the internal resistance of the VRLA cells occurs in the SOC values between 0–0.2 and 0.8–1.0. This suggests that the operation of the cells in this range of SOC values may lead to deleterious internal heating. The charge-transfer resistances of the positive ($R_{t,2}$) and negative ($R_{t,1}$) electrodes of these VRLA cells are found to be minimum over the SOC range between 0.2–0.8 and it would be therefore preferable to limit the operation of these cells in this range of SOC values. Since the $R_{t,1}$ value is substantially lower than $R_{t,2}$, it is suggested that the performance of the VRLA cells employed in this study can be improved by the electrocatalysis of the $PbO_2/PbSO_4$ electrode reaction. The present method can also be effectively used for monitoring the SOC values of the VRLA cells by measuring the variation in the interfacial capacitance of the positive plates ($C_{d,2}$).

References

[1] A.J. Salkind, J.J. Kelly, A.G. Cannone, in: D. Linden, (Ed.), Handbook of Batteries, Mc-Graw Hill, New York, 1995, pp. 24.1–24.89.
[2] R.O. Hammeal, A.J. Salkind, D. Linden, in: D. Linden, (Ed.), Handbook of Batteries, Mc-Graw Hill, New York, 1995, pp. 25.1–25.39.
[3] D. Berndt, Maintenance Free Batteries, Wiley, New York, 1993.
[4] T.R. Crompton, Battery Reference Book, Butterworth, London, 1990.
[5] K.R. Bullock, J. Power Sources 51 (1994) 1.
[6] M.W. Kniveton, J. Power Sources 53 (1995) 149.
[7] G.J. May, J. Power Sources 59 (1996) 147.
[8] V. Ganesh Kumar, N. Munichandraiah, A.K. Shukla, J. Appl. Electrochem. 27 (1997) 43.
[9] V. Ganesh Kumar, N. Munichandraiah, A.K. Shukla, J. Power Sources 63 (1996) 203.
[10] S.A. Ilangovan, S. Sathyanarayana, J. Appl. Electrochem. 22 (1992) 456.
[11] S.A. Ilangovan, PhD thesis, Indian Inst. Sci., Bangalore, 1991.
[12] F. Beck, in: A.T. Kuhn, (Ed.), Electrochemistry of Lead, Academic Press, London, 1979.
[13] P. Delahay, M. Pourbaix, P.V. Rysselberghe, J. Electrochem. Soc. 98 (1951) 57.
[14] K. Vijayamohanan, A.K. Shukla, S. Sathyanarayana, J. Electroanal. Chem. 295 (1990) 59.
[15] S.Ya. Volosava, Z.A. Lofa, T.G. Stepina, Electrokhimiya 13 (1977) 393.
[16] R.T. Barton, M. Huges, S.A.G.R. Karunathilaka, N.A. Hampson, J. Appl. Electrochem. 15 (1985) 399.
[17] J.C. Amphlett, E.H. de Oliveira, R.F. Mann, P.R. Roberge, A. Rodrigues, J.P. Salvador, J. Power Sources 65 (1997) 173.
[18] T. Higginson, K. Peters, in: L.J. Pearce (Ed.), Power Sources 11, International Power Sources Symposium Committee, Leatherhead, UK, 1986, p. 21.